Int. J. Electrochem. Sci., 13 **(2018)** 1367 – 1375, doi: 10.20964/2018.02.31

International Journal of
ELECTROCHEMICAL
SCIENCE
www.electrochemsci.org

Electrodeposition of PANI/MWCNT Coatings on Stainless Steel and Their Corrosion Protection Performances

Wei Li

Department of capital construction of Xinxiang University, Xinxiang, Henan, 453000, P.R. China
E-mail: weili_1912@163.com

Received: 9 September 2017 / *Accepted:* 19 October 2017 / *Published:* 28 December 2017

When used under corrosive conditions as a coating material, nanostructured composites demonstrated higher sensitivity and better performance. In this work, mild steel (MS) structures were effectively protected through enhancement of the mechanical and corrosive performances of polyaniline (PANI) coatings using functionalized carbon nanotubes (CNTs). Fourier transform infrared (FTIR) spectroscopy and cyclic voltammetry (CV) were used to measure the coatings. Electrochemical impedance spectroscopy (EIS) and the Tafel test were used to study the corrosion performance of polymer-coated MS configurations in a highly corrosive 0.5 M HCl solution. For all immersion times, the corrosion resistance of the PANI/MWCNT was found to be higher than that of other coatings.

Keywords: Carbon nanotubes; Polyaniline; Electrodeposition; Corrosion protection; Nanocomposite

1. INTRODUCTION

Conducting polymers can be easily prepared and widely applied because of their distinct biological, chemical, optical, environmental, thermal, and electrical features, and they have gained substantial attention recently in scientific and technological fields [1-5]. For the corrosion protection of metals including copper, aluminum, iron, stainless steel, and mild steel (MS), conducting polymers have played a vital role over the past decade [6-10]. The electrochemical synthesis of polyaniline (PANI) has been proved to effectively inhibit the corrosion of pure iron, stainless steel and MS [11-14].

Notably, nanocomposites consisting of carbon nanotubes (CNTs) and conductive polymers have gained great attention recently because of the synergistic effects of these two classes of materials. As a conductive polymer (CP), PANI is highly environmentally stable, redox reversible, conductive, and aqueous soluble, and its color can change swiftly at different potentials, making it a popular material [15-18]. Unfortunately, PANI can shrink, break, and crack under extreme conditions,

suggesting an undesirable mechanical stability; these disadvantages are associated with volumetric changes of the polymer in the process of charging and discharging [10, 19-21]. Another drawback lies in the high porosity of PANI when used to protect against corrosion as a coating material because it can induce corrosion on metal coating interfaces through enhanced electrolyte uptake through its porous structure. The results show that it is necessary for the PANI to be combined with other functional materials to generate composites for better performance and more extensive applications [22-24].

Gupta and Miura [25] proposed the fabrication of distinct supercapacitors based on composite PANI-CNT films made by electrochemical deposition. Karim et al. [26] reported the complexity of PANI-coated nanotubes. The thermal stability and conductivity of these sophisticated nanotubes were lower compared with those of CNT and were higher than PANI. However, CNTs were difficult to process and showed insolubility in most solvents. Hence, increasing the solubility is essential to increase their potential applications. CNTs could be functionalized through an oxidization process involving ultrasonic treatment in a mixture of sulfuric acid and concentrated nitric acid, which leads to the attachment of the sidewalls and ends of the as-prepared CNTS to carboxyl groups.

The present work used a potentiodynamic method for the electrosynthesis of the PANI/MWCNT coatings on passivated mild steel (MS) surfaces. EIS and potentiodynamic polarization were used to study the corrosion performance of PANI/MWCNT-coated MS electrodes in 0.5 M HCl.

2. EXPERIMENTS

2.1. Chemicals

COOH-functionalized nanotubes (c-MWNTs; inner diameter, 8–15 nm; outer diameter, 3–5 nm; length, 10–50 μm) were provided by Shenzheng Nano Tech. Lab. Corporation. All other reagents (hydrochloric acid, NaOH, H_2SO_4, Na_2SO_4) were provided by Merck and were used as received. A NaOH or H_2SO_4 aqueous solution (0.1 M) was added to adjust the solution pH. Deionized water was used to prepare all the test solutions.

2.2. Apparatus and techniques

A PerkinElmer 65 spectrophotometer was used for the FT-IR characterizations. An Ivium CompactStat (Ivium Technologies B.V, The Netherlands) electrochemical analyzer was used for electrochemical experiments. For Tafel experiments, an anodic sweep ±0.200 V range of the open circuit potential (E_{OCP}) was performed in 0.5 M HCl (scan rate: 1 mV/s). Prior to the Tafel measurements, the bare MS and polymer-modified MS configurations were held in the solution until a stable value was obtained for the $E_{OCP.}$ IviumSoft software (version 1.832) was used for the automatic calculation of the corrosion rate parameters. The EIS experiment was carried out at the E_{OCP} of the substrates at varying immersion times in 0.5 M HCl, and other parameters were presented as follows:

amplitude, 5 mV; frequency range, 10^5 to 0.1 Hz. Based on the EIS experiments from the obtained data, ZView 3.2c software was used to obtain the equivalent circuit models. The electrochemical performance of the bare and coated configurations was investigated using linear scanning voltammetry (LSV).

2.3. Electrosynthesis of PANI and PANI/MWCNTs nanocomposites

The electrochemical synthesis of PANI/c-MWCNTs nanocomposites was carried out at ambient temperature using a potentiostat. After the dispersion of a certain amount of MWCNTs into sulfuric acid (50 mL, 0.5 M) at ambient temperature for 1 h, the aniline monomer was dissolved in the electrolyte solution and ultrasonically stirred for 5 min. A stainless-steel electrode was used for the electrochemical polymerization (200 seconds), at an applied potential *vs.* SCE (reference electrode) kept constant at +0.95 V. The counter electrode was a graphite sheet. To maintain a continuous dispersion of MWCNTs in contact with the surface of the electrode, the electrolyte solution adjacent to the working electrode area was magnetically stirred at low speed during the polymerization process. This was followed by rinsing this electrode using distilled water. Afterwards, the as-prepared electrode was transferred to 0.5 M H_2SO_4. PANI without MWCNTs was achieved under the same conditions without a dispersion of MWCNTs.

3. RESULTS AND DISCUSSION

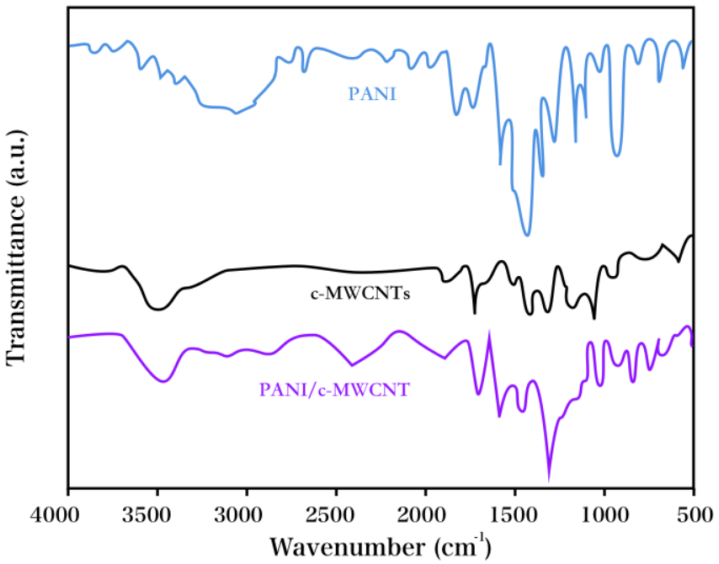

Figure 1. FTIR spectrum of PANI, c-MWCNTs and the PANI/c-MWCNTs nanocomposite.

PANI, c-MWCNTs and PANI/c-MWCNTs nanocomposites were characterized via the FTIR profiles in Fig. 1. For PANI, characteristic peaks at *ca.* 1558 and 1492 cm^{-1} were observed in its FTIR spectrum, which indicated the quinoid and benzenoid ring vibrations respectively [27, 28]. In the PANI

ring, the C–H and N–H stretching vibrations were reflected by the absorptions at *ca.* 2961 and 3442 cm^{-1} [29]. The as-assigned peaks suggest the polyaniline property of the obtained product. The peaks observed at 1703 and 3432 cm^{-1} corresponded to the C=O and O–H stretching vibrations of carboxyl groups in the c-MWCNTs, respectively. Furthermore, the C–O stretching vibration was reflected by the peak observed at 1043 cm^{-1} [30, 31]. As confirmed by the results of the FTIR experiments, PANI/c-MWCNTs nanocomposites were formed through an electropolymerization process.

For the coatings, CV experiments were carried out in a blank solution (0.3 M HCl solution) to investigate their electrochemical features, and the feature comparison between those and the bare electrode was presented in Fig. 2. Iron dissolution occurred at *ca.* −0.5 V for the bare configuration, which produced Fe^{2+} ions during the first anodic sweep. A passive layer of iron (II) oxalate dihydrate ($FeC_2O_4 \cdot 2H_2O$) was formed on the surface of the electrode through the reaction between the above ions and oxalate ions. When the applied potential was *ca.* −0.2 V, the current reached the maximum value, which then decreased to *ca.* −0.1 V since a layer of $FeC_2O_4 \cdot 2H_2O$ formed; almost no current variation was found until the iron (III) species was formed [32, 33]. An apparent oxidation peak was observed at *ca.* 0.20 V during the reverse sweep. When the applied potential was more negative at 0.1 V, the repassivation peak intensity significantly decreased in the presence of the PANI coating, whereas the PANI/c-MWCNTs nanocomposite coating showed no repassivation peak.

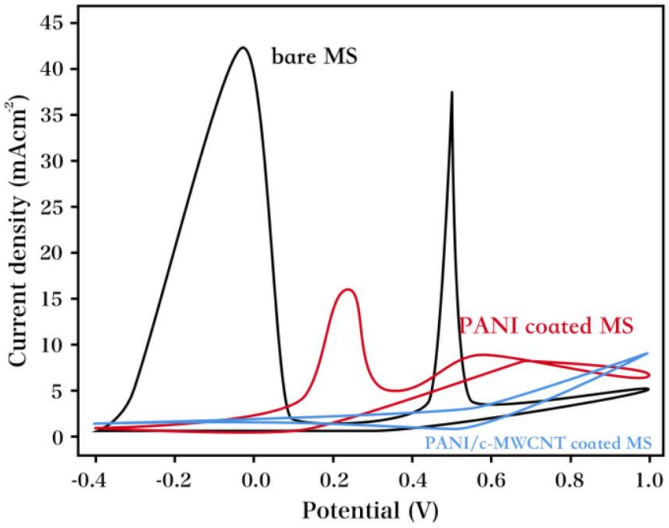

Figure. 2. Cyclic voltammograms of bare MS, PANI- and PANI/c-MWCNTs-coated MS in 0.3 M HCl.

For the bare MS, passivated MS, PANI-modified MS and PANI/c-MWCNTs-modified MS electrodes, linear anodic polarization characterizations were carried out in 0.5 M H_2SO_4 , as shown in Fig. 3. For the bare MS configuration, the oxidation current recorded in the range from −0.5 to 0.45 V corresponded to the dissolution of iron. After the passivation of MS, a decrease was found in both the dissolution current and the corresponding potential interval. For the PANI and PANI/c-MWCNTs nanocomposite-coated surfaces, the dissolution currents were lower, offering enhanced corrosion

protection in acidic media. Compared with the passivated MS surface, the PANI and PANI/c-MWCNTs nanocomposite coatings showed decreased dissolution currents, and the potential intervals were significantly narrower. In addition, PANI/c-MWCNTs nanocomposite coating exhibited the lowest dissolution current.

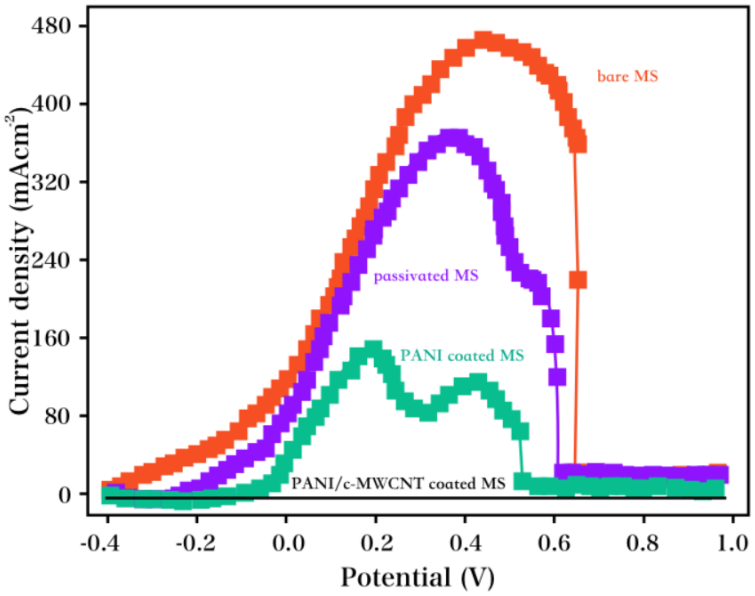

Figure 3. Linear anodic potentiodynamic polarization curves of bare MS, passivated MS, PANI-coated MS and PANI/c-MWCNTs-coated MS.

The bare MS, PANI-modified MS and PANI/c-MWCNTs-modified MS were further characterized in 0.5 M HCl via Tafel curves, as shown in Fig. 4. The linear segments of the recorded Tafel patterns were extrapolated to obtain the corrosion current density (i_{corr}), corrosion potential (E_{corr}), and the anodic and cathodic Tafel constants (β_a, β_c). Table 1 shows the polarization parameters of the bare MS, PANI-modified MS and PANI/c-MWCNTs-modified MS. When the potential increased as high as -534 mV, the PANI/c-MWCNTs-modified MS showed no breakdown potential, indicating that this sample was highly resistant to local corrosion. In addition, the Stern–Geary equation was used to calculate the polarization resistance (R_p) [34]. Nevertheless, the i_{corr} values must have been affected by the steel corrosion and redox process of the electroactive conducting polymer [35]. The results confirm that i_{corr} represented the exchange in the current density values [36]. When the solutions were acidic, iron was dissolved during the anodic reaction, followed by oxidization to a higher valence state. Due to the electrons received from the metal during the cathodic reaction, a decrease in the species dissolved in solution was found, including oxygen, hydrogen ions, etc. Initially, the cathodic reaction occurred on the surface of the metal, which was then transferred to the polymer/electrolyte interface; this transfer resulted from the conduction property of the electroactive polymers [37]. Therefore, for differently synthesized coatings, the extent of E_{corr} change varies. Compared with the bare configuration, the PANI-coated MS configuration showed an E_{corr} shift in the positive direction, whereas other polymer-coated steel electrodes showed an E_{corr} shift in the negative

direction. The results showed that the PANI/c-MWCNTs-coated MS exhibited a maximal shift when the potential was *ca.* 0.05 V. There are two possible causes for the above shifts: the insertion of the anions into the polymer structures as the counter ions, and/or the electroactivity of protective polymer coatings.

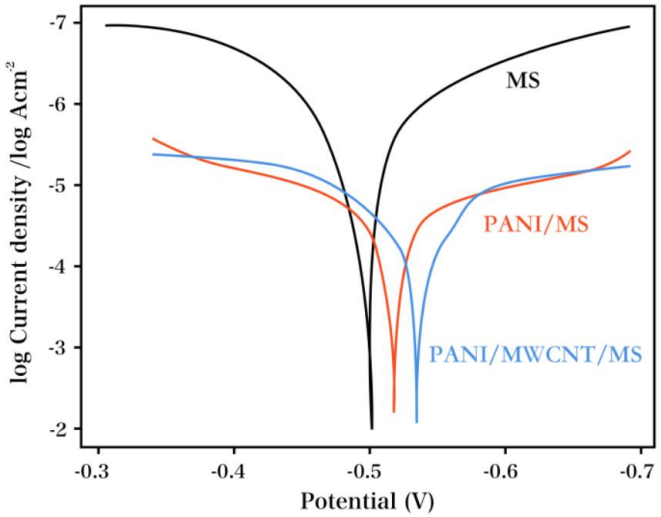

Figure 4. Tafel extrapolation curves of bare MS, PANI-modified MS and PANI/c-MWCNTs-modified MS in 0.5 M HCl.

Table 1. Electrochemical polarization parameters for the bare MS, PANI-modified MS and PANI/c-MWCNTs-modified MS.

Sample	E_{corr} (mV)	I_{corr} (mA/cm^2)	b_a (mV/dec)	b_c (mV/dec)
Bare MS	-507	3.41	87	100
PANI modified MS	-522	3.21	82	101
PANI/c-MWCNTs modified MS	-534	2.99	79	98

Nyquist profiles were recorded for the bare MS electrode after it was immersed in 0.5 M HCl for 15 min and 6 h, respectively, as shown in Fig. 5A. The obtained profiles can be fitted with a semicircle ascribed to corrosion processes that occurred on the MS surface. As the exposure time was increased, the R_{ct} values decreased. The results showed that the presence of chloride ions led to the dissolution of iron in the corrosive solution; and as the exposure time was prolonged, the amount of soluble species was found to increase [38]. The protection efficiency (PE%) values for the coatings were calculated from the EIS data and are given in Table 2.

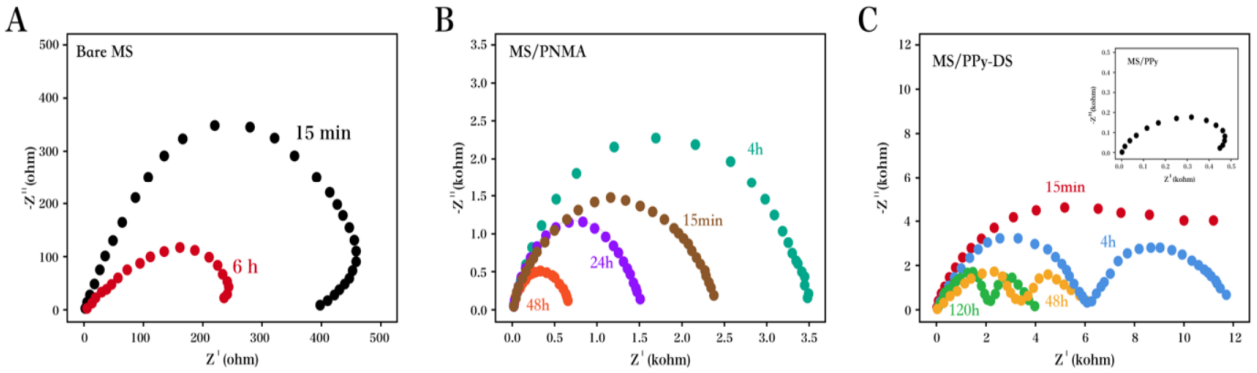

Figure 5. (A) Nyquist profiles recorded for bare MS electrode after immersion in 0.5 M HCl for 15 min and 6 h, respectively. (B) Nyquist profiles recorded for PANI-modified MS after immersion in 0.5 M HCl for 15 min, 4 h, 24 h and 48 h, respectively. (C) Nyquist profiles recorded for PANI/c-MWCNTs-modified MS after immersion in 0.5 M HCl for 15 min, 4 h, 48 h and 120 h, respectively.

Table 2. The results obtained by EIS for bare, PANI-modified and PANI/c-MWCNTs-modified MS electrodes.

Sample	Rs (Ω)	CPE_c $(\mu F)^{n1}$	n1	Rpore (Ω)	CPE_{dl} $(\mu F)^{n2}$	n2	Rct (Ω)	R_p (Ω)	PE%
Bare MS									
15 min	7.455	-	-	-	36.54	0.889	485.3	-	-
6 h	7.985	-	-	-	377.5	0.821	177.5	-	-
PANI modified MS									
15 min	8.224	6.188	0.9355	201.8	6.114	0.6522	2607.5	2304.6	96.5
4 h	7.403	6.652	0.9306	172.6	7.662	0.7051	2541.5	3500.4	94.3
24 h	8.488	6.995	0.9210	166.2	15.74	0.7238	1425.6	1718.5	91.1
48 h	10.21	7.632	0.8911	221.4	176.2	0.7514	264.8	784.5	88.6
PANI/c-MWCNTs modified MS									
15 min	4.395	0.7824	0.7806	455.2	135.6	0.3112	6851	15200	95.7
4 h	4.055	0.2776	0.5114	3114	36.77	0.5420	5411	11204	96.3
48 h	4.705	0.2804	0.3541	4021	38.52	0.6633	3574	6050	92.5
120 h	22.24	0.3541	0.4155	4451	40.06	0.6417	3022	5325	91.2

Nyquist profiles were also recorded for PANI-modified MS after immersion in 0.5 M HCl for 15 min, 4 h, 24 h and 48 h, respectively, as shown in Fig. 5B. The obtained profiles were fitted with a semicircle. Compared with the bare MS electrode, the PANI-modified MS configuration showed increased $R_{p,c}$, and the CPE_{dl} values were vice versa. The increase in $R_{p,c}$ values confirmed that a stable passive layer was formed at the interface of polymer and electrode. In the presence of polymer coatings, diffuse steel was considered the only corrosive constituents. The PANI-modified MS showed an increase in the $R_{p,c}$ values up to 4 h, followed by a gradual decrease. This may result from the redox processes for PANI polymer in the acidic corrosive solution.

Nyquist profiles were further recorded for the MS/PPy-DS electrode and the PANI/c-MWCNTs-modified MS after immersion in 0.5 M HCl for 15 min, 4 h, 48 h and 120 h, respectively, as shown in Fig. 5C. A general decrease was observed for the $R_{p,c}$ value with increased immersion time. For the corrosion resistances, the maximal $R_{p,c}$ value of the PANI coating was lower compared with the minimal $R_{p,c}$ value of the PANI/MWCNT coating.

4. CONCLUSIONS

The present work proposed an electrodeposition strategy for the electrochemical synthesis of the PANI/c-MWCNTs on the surface of MS, and their corrosion behaviors in 0.5 M HCl were compared with those of nanocomposite coatings presented herein. Compared with EIS techniques, the Tafel extrapolation showed a consistency in the results of the protection behavior. It was found that these nanocomposite coatings provided effective protection for mild steel against corrosion, despite the relatively high corrosiveness of the medium (acidic solution) concentration. The nanocomposite coatings effectively protected against corrosion through the following processes: during electrodeposition, a stable interface formed between the MS configuration and the polymer to effectively block the corrosive ions. Considering the electrical conductivity of the polymer, electron transfer was between the corrosive solution and the metal surface was inhibited.

References

1. J. Lee, P. Lee, H.B. Lee, S. Hong, I. Lee, J. Yeo, S.S. Lee, T.S. Kim, D. Lee and S.H. Ko, *Advanced Functional Materials*, 23 (2013) 4171.
2. J.H. Yim, S.-y. Joe, C. Pang, K.M. Lee, H. Jeong, J.-Y. Park, Y.H. Ahn, J.C. de Mello and S. Lee, *ACS nano*, 8 (2014) 2857.
3. C. Janáky and C. Visy, *Analytical and bioanalytical chemistry*, 405 (2013) 3489.
4. K.F. Babu, S.P.S. Subramanian and M.A. Kulandainathan, *Carbohydrate polymers*, 94 (2013) 487.
5. Y. Yang, S. Li, W. Yang, W. Yuan, J. Xu and Y. Jiang, *ACS applied materials & interfaces*, 6 (2014) 13807.
6. U. Riaz, C. Nwaoha and S. Ashraf, *Progress in Organic Coatings*, 77 (2014) 743.
7. A. Mostafaei and F. Nasirpouri, *Progress in Organic coatings*, 77 (2014) 146.
8. P.P. Deshpande, N.G. Jadhav, V.J. Gelling and D. Sazou, *Journal of Coatings Technology and Research*, 11 (2014) 473.
9. M. Deyab, *Journal of Power Sources*, 268 (2014) 50.
10. M. Sababi, J. Pan, P.-E. Augustsson, P.-E. Sundell and P.M. Claesson, *Corrosion Science*, 84 (2014) 189.
11. A. Ali Fathima Sabirneeza and S. Subhashini, *Journal of Applied Polymer Science*, 127 (2013) 3084.
12. C. Janáky and K. Rajeshwar, *Progress in Polymer Science*, 43 (2015) 96.
13. S. Jafarzadeh, P.M. Claesson, P.-E. Sundell, E. Tyrode and J. Pan, *Progress in organic coatings*, 90 (2016) 154.
14. A. Kalendová, D. Veselý, M. Kohl and J. Stejskal, *Progress in Organic Coatings*, 78 (2015) 1.
15. A.M. Kumar and Z.M. Gasem, *Progress in Organic Coatings*, 78 (2015) 387.
16. X. Li, J. Shen, W. Sun, X. Hong, R. Wang, X. Zhao and X. Yan, *Journal of Materials Chemistry A*, 3 (2015) 13244.

17. A.A. Farag, K.I. Kabel, E.M. Elnaggar and A.G. Al-Gamal, *Corrosion Reviews*, 35 (2017) 85.
18. J. Pagotto, F. Recio, A. Motheo and P. Herrasti, *Surface and Coatings Technology*, 289 (2016) 23.
19. Z.-s. Yin, T.-h. Hu, J.-l. Wang, C. Wang, Z.-x. Liu and J.-w. Guo, *Electrochimica Acta*, 119 (2014) 144.
20. M.K. Kim, K.S. Sundaram, G.A. Iyengar and K.-P. Lee, *Chemical Engineering Journal*, 267 (2015) 51.
21. H. Wei, D. Ding, S. Wei and Z. Guo, *Journal of Materials Chemistry A*, 1 (2013) 10805.
22. H. Li, X. Lu, D. Yuan, J. Sun, F. Erden, F. Wang and C. He, *Journal of Materials Chemistry C*, (2017)
23. Y. Jafari, S.M. Ghoreishi and M. Shabani-Nooshabadi, *Journal of Polymer Research*, 23 (2016) 91.
24. M. Ates and E. Topkaya, *Progress in Organic Coatings*, 82 (2015) 33.
25. V. Gupta and N. Miura, *Electrochimica acta*, 52 (2006) 1721.
26. M.R. Karim, C.J. Lee, Y.-T. Park and M.S. Lee, *Synthetic metals*, 151 (2005) 131.
27. Q. Yu, X. Li, L. Zhang, X. Wang, Y. Tao and X. Wang, *Journal of Polymer Materials*, 32 (2015) 411.
28. J. Cheng, B. Zhao, S. Zheng, J. Yang, D. Zhang and M. Cao, *Applied Physics A*, 119 (2015) 379.
29. R.V. Gonçalves, M.L. Zanini, J.A. Malmonge, L. Bonnaud and N.R. de Souza Basso, *Materials Letters*, 185 (2016) 327.
30. M. Khairy and M. Gouda, *Journal of advanced research*, 6 (2015) 555.
31. W. Zheng, S. Nayak, W. Yuan, Z. Zeng, X. Hong, K.A. Vincent and S.C.E. Tsang, *Chemical Communications*, 52 (2016) 13901.
32. J. Camalet, J. Lacroix, S. Aeiyach, K. Chane-Ching and P. Lacaze, *Synthetic Metals*, 93 (1998) 133.
33. W. Su and J.O. Iroh, *Electrochimica acta*, 44 (1999) 3321.
34. M. Stern, *Journal of The Electrochemical Society*, 104 (1957) 751.
35. C.K. Tan and D.J. Blackwood, *Corrosion Science*, 45 (2003) 545.
36. P. Ocon, A. Cristobal, P. Herrasti and E. Fatas, *Corrosion science*, 47 (2005) 649.
37. A.J. Dominis, G.M. Spinks and G.G. Wallace, *Progress in Organic Coatings*, 48 (2003) 43.
38. T. Tüken, A. Özyılmaz, B. Yazıcı and M. Erbil, *Applied surface science*, 236 (2004) 292